

Chapter 9

Electrochemistry, Batteries, and Fuel Cells

9.1 Introduction

Electrochemistry is concerned with the effect of electrical voltages and currents on chemical reactions (*ionics*) and chemical changes which produce the voltages and currents (*electrodics*). This is illustrated in Table 9.1 where ionics is governed by Faraday's laws, whereas electrodics is determined by the Nernst equation.

9.2 Ionics

Faraday's laws of electrolysis are:

1. The mass of material formed at the electrodes is proportional to the quantity of electricity passed through the solution.
2. For a fixed quantity of electricity passed through a solution, the masses of different materials formed (or dissolved) at the electrode are proportional to their equivalent weight, which is the atomic mass/electron charge, Z .
3. The charge on the electron is 1.60219×10^{-19} coulombs. Hence, one mole of electrons (6.02214×10^{23}) represents $1.60219 \times 10^{-19} \times 6.02214 \times 10^{23} = 9.6486 \times 10^4$ coulombs/mol which is called a Faraday (\mathcal{F}) and usually rounded off to 96,500 coulombs. A coulomb, Q , is equal to $1 \text{ amp} \times 1 \text{ s}$, and $26.80 \text{ amp-h} = 1 \mathcal{F}$

$$Q = It \tag{9.1}$$

where I is the current in amperes and t is the time in seconds.

Example 9.1

How much silver would be electrodeposited by a current of 6.0 amp for 3 h from a solution of AgNO_3 ?

Answer: The atomic mass of silver is 107.87 g/mol. The charge on silver is +1 ($Z = 1$), and this means that $1 \mathcal{F}$ would deposit 107.87 g. We must now determine the number of coulombs, Q , which were passed through the solution.

Table 9.1 The classification of electrochemical systems

Ionics	Electrodics
Faraday's law	Nernst equation
Current flow causes reaction to occur	Reactions cause voltage to develop and current to flow
Electrolysis	Batteries
Electrodeposition	Fuel cells
Electrochemical machining	Corrosion protection
Battery charging	

$$Q = It = 6.0 \text{ amp} \times 3 \text{ h} \times 60 \text{ min/h} \times 60 \text{ s/min} = 64,800 \text{ amp.s} \quad (9.2)$$

96,500 C would deposit 107.87 g of Ag and 1 C would deposit 107.87/96,500 g of Ag. Hence, 64,800 C would deposit $64,800 \times 107.87/96,500$ g of Ag, or 72.43 g of silver would be deposited.

Example 9.2

During the 4.0 h electrodeposition of copper from a copper sulfate (CuSO_4) solution, 140.0 g of Cu was deposited. What was the current flowing through the cell?

Answer: The atomic mass of copper is 63.55 g/mol. Since the charge on the copper in the solution, Cu^{2+} , is +2, then the equivalent weight is 63.55/2 g. Hence, 1 \mathcal{F} would deposit 63.55/2 g Cu. Since 140.0 g of Cu was deposited, the quantity of current which flowed through the cell is $140.0/63.55/2$ or 4.406 \mathcal{F} .

$$Q = It$$

$$I = \frac{Q}{t} = \frac{4.406 \times 96,500}{4 \times 3,600} \text{ amp} = 29.53 \text{ amp}. \quad (9.3)$$

Example 9.3

An alloy of tin and lead is deposited from a solution of $\text{Sn}(\text{NO}_3)_2$ and $\text{Pb}(\text{NO}_3)_2$. What is the percentage of tin in the alloy if 35.00 g of alloy is deposited when 3.00 amp of current is passed through the solution for 4.00 h?

Answer: The quantity of electricity Q passed through the solution is given by:

$$Q = It = 3.00 \times 4.00 \times 3,600 = 43,200 \text{ C}$$

96,486 C liberates 1 equivalent weight, 1 C liberates 1/96,486 equivalent weights, and 43,200 C liberates $43,200/96,486$ equivalent weights, that is, a total of 0.448 equiv. If M is the mass of Sn in the deposit, then 35.00 M is the mass of Pb.

The equivalent weight of Sn is

$$\frac{118.7}{2} = 59.35 \text{ g/eq.}$$

The equivalent weight of Pb is

$$\frac{207.2}{2} = 103.6 \text{ g/eq.}$$

Hence, the number of equivalents of Sn in the deposit is

$$\frac{M}{59.35},$$

and the number of equivalents of Pb in the deposit is

$$\frac{35.00 - M}{103.6}.$$

Thus,

$$\frac{M}{59.35} + \frac{35.00 - M}{103.6} = 0.448.$$

Solving for M

$$\begin{aligned} 103.6M + 2,077 - 59.35M &= 2,754 \\ 44.2M &= 677 \\ M &= 15.3 \text{ gSn} \\ 35.00 - M &= 19.7 \text{ gPb} \end{aligned}$$

Percentage of Sn in the alloy is

$$\frac{15.3}{35.00} \times 100 = 43.7\%.$$

Example 9.4

High purity gases are often prepared by electrolysis. It is desired to produce O_2 at $25^\circ C$ and 800 torr at a flow rate of $75.0 \text{ cm}^3/\text{min}$. What current would be required for the electrolysis cell which consists of aqueous NaOH solution and nickel electrodes?

Answer: Using $PV = nRT$, we see that a flow rate of $75.0 \text{ cm}^3/\text{min}$ corresponds to a flow rate of

$$\begin{aligned} n &= PV/RT = \{800 \text{ torr}/760 \text{ torr/atm}\} \\ &\quad \times 75.0 \text{ mL/min} \times (82.06 \text{ mL.atm/K.mol})^{-1} \times [298 \text{ K}]^{-1} \\ n &= 3.228 \times 10^{-3} \text{ mol/min} \end{aligned}$$

For O_2 gas, 1 mole corresponds to 4 equivalents. Thus, this flow rate corresponds to

$$4 \times 3.228 \times 10^{-3} \text{ equiv./min}$$

or

$$\frac{4 \times 3.228 \times 10^{-3}}{60} \text{ equiv./s,}$$

that is, \mathcal{A}/s . Thus,

$$\text{current required} = \frac{4 \times 3.228 \times 10^{-3} \times 96,485}{60} \text{ C/s}$$

$$I = 20.77 \text{ C/s}$$

$$I = 20.77 \text{ amp}$$

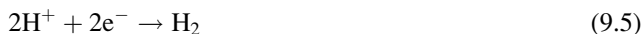
One mole of H_2 prepared by the electrolysis of water would require $2\mathcal{F}$, whereas 1 mole of O_2 would require $4\mathcal{F}$. The electrolysis of Al_2O_3 in cryolite (Na_3AlF_6) requires $3\mathcal{F}$ for each mole of Al (27 g). This is very energy intensive, and a tonne of aluminum uses over 15,000 kW. Some effort (though unsuccessful) has been made to convert Al^{3+} to Al^{+1} in order to save on electrical energy by electrolyzing Al^+ instead of Al^{3+} .

9.3 Electrolysis and Electrodeposition of Metals

When an increasing DC voltage is applied to a solution of metal ions, the metal, in some cases, will begin to deposit the deposition material at the cathode at a minimum voltage. This is illustrated as D in Fig. 9.1. The deposition potential depends on the metal, the surface, the current density, the concentration of the metal, and other ions in solution. The electrodeposition or electroplating reaction



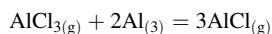
is most common for metals such as Au, Ag, Pb, Cd, Zn, Cr, Ni, Cu, and Sn. Two or more metals can also be deposited to form alloys. If the voltage is too high, then hydrogen will be evolved:



The theoretical minimum voltage required for the electrolysis of water is 1.23 V at 25°C . However, the process has an activation energy which is referred to as the overvoltage or polarization which depends on the current, temperature, and materials used for the electrodes. Some typical overvoltages are given in Table 9.2.

The industrial preparation of hydrogen by the electrolysis of water on nickel electrodes requires a voltage of more than 1.50 V ($1.23 \text{ V} + 0.210 \text{ V} + 0.060 \text{ V}$) since it is necessary to add the RI drop (due to the internal resistance of the electrolyte). However, at very high current densities, the polarization is much higher, and higher temperatures are used to reduce the excess power

¹ The ground state electronic configuration of Al is $1s^2 2s^2 2p^6 3s^2 3p^1$, and it would be expected for Al to have a (+1) oxidation state. This is in fact the case, and at high temperatures, the reaction.



occurs. However, attempts to electrolyze AlCl have so far proved to be unsuccessful.

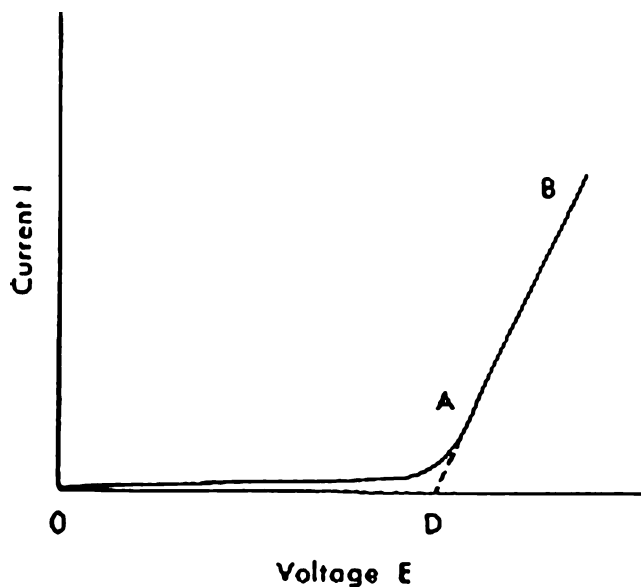


Fig. 9.1 Typical current–voltage plot for an electrolyte solution. *A* start of deposition, *A–B* linear segment of plot, *D* extrapolated deposition potential

Table 9.2 Overvoltage (mV) in water electrolysis, 25°C

Metal surface	Cathode polarization dilute H ₂ SO ₄	Anode polarization dilute KOH
Platinized platinum	5	250
Smooth platinum	90	450
Palladium	~ 0	430
Gold	20	530
Silver	150	410
Nickel	210	60
Lead	640	310
Cadmium	480	530
Mercury	780	–

requirements. The overvoltage encountered in the electrodeposition of a metal can be associated with the various steps by which the metal in solution, for example, Cu^{2+} , becomes the atom in a copper lattice.

The various steps in the overall mechanism are:

1. Cu^{2+} (hydrated in solution) diffuses to the cathode.
2. Cu^{2+} (hydrated) at electrode is transferred to the cathode surface.
3. Cu^{2+} (partially hydrated and adsorbed onto the surface), the ad ion, diffuses across the electrode surface to a crystal building site.
4. Cu^{2+} (adsorbed at a crystal building site) becomes a part of the lattice.
5. $[\text{Cu}^{2+} + 2\text{e}^-]$ occurs, and Cu is part of the metal.

The sequence of relative importance is $2 > 3 > 4 > 1 > 5$ with step 2 being the slowest step or rate-controlling process.

9.4 Electrochemical Machining

Electrolysis, with an anode that dissolves under controlled conditions, is the basis of electrochemical machining (ECM). High-strength metals such as Nimonic alloys (nickel with Al, Ti, and Mo) used in the aircraft industry resist deformation even at high temperatures and are exceedingly difficult to machine by the normal cutting process because of the limitations and expense of tool materials. In ECM, the metal alloy does not determine the rate or characteristics of the dissolution process, and hard tough metals can be dissolved as readily as soft metals. Only the current density (amp/cm²) determines the rate of machining where approx. 5×10^{-3} mm/min can be removed at a current density of 0.3 amp/cm². The additional advantage of ECM is the absence of mechanical and thermal stress usually associated with conventional machining.

A schematic representation of a typical ECM apparatus is shown in Fig. 9.2 and consists of a workpiece to be machined (the anode), a properly shaped cathode tool which is movable and maintains a constant gap with the workpiece. The electrolyte flows between the two electrodes, removing the products of electrolysis as well as heat. The power supply furnishes the high currents necessary to dissolve the anode.

9.4.1 The Cathode

The cathode is a tool shaped to conform to the desired cut in the workpiece. The tool is usually made from copper, steel, or alloy and insulated on the sides to give directed current lines. The tool is moved during electrolysis to maintain a constant small gap (about 0.25 mm) between the electrodes to reduce the voltage required.

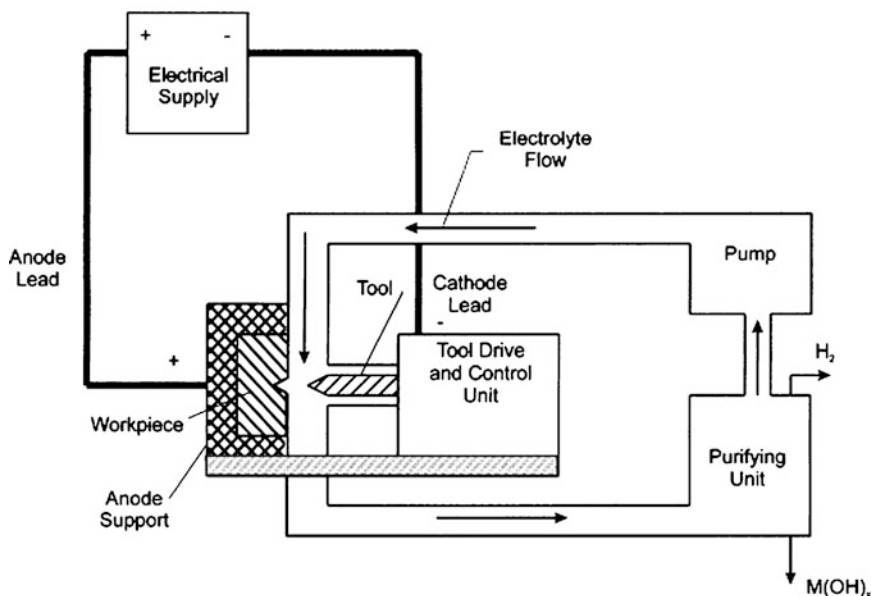


Fig. 9.2 Schematic diagram of an ECM unit

Table 9.3 Composition of various iron-base alloys^a

Iron-base alloy	Element (%)							
	C	Cr	Mo	Mn	Si	P	S	Ni
SCM 3	0.35	1.1	0.2	0.7	0.25	0.03	0.03	—
SKD 11	1.5	12.0	1.0	—	—	—	—	—
SNC2	0.3	0.8	—	0.5	0.2	0.03	0.03	2.7
SUS 304	0.08	17.5	—	20	1.0	0.045	0.03	9.5
Inconel 718	0.06	18.26	2.93	0.11	0.13	0.0001	0.003	51.85

^aIron is the remaining element making up the alloy's 100%

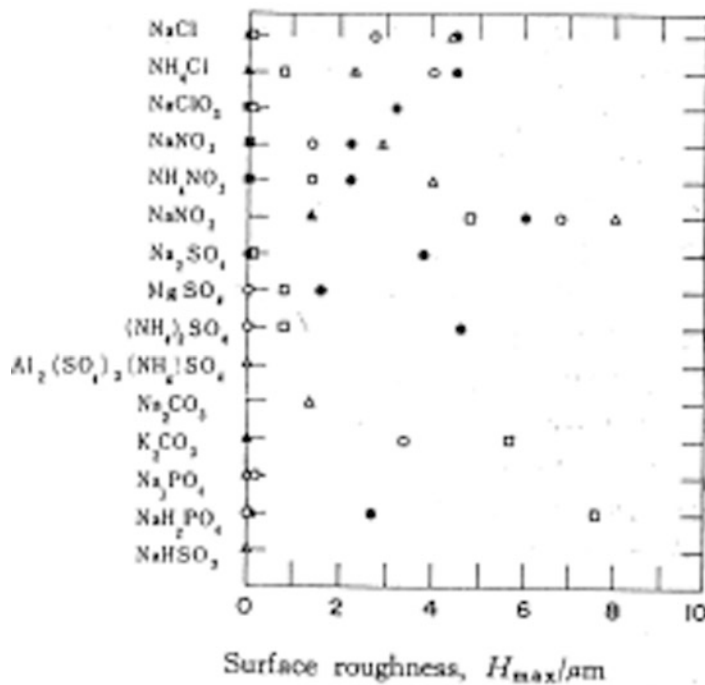


Fig. 9.3 Surface roughness of steels (see Table 9.3) obtained in various electrolytes. O SCM 3, ● SKD 11, Δ SNC 2, ▲ SUS 304, □ Inconel 718

9.4.2 The Electrolyte

The purpose of the electrolyte is to provide a conducting medium, and at the same time, it must not corrode the cathode tool. The cheapest material commonly used is sodium chloride (NaCl) at about 30% by weight. In some cases, additives such as alcohols, amines, thiols, and aldehydes are used to inhibit stray currents, which results in overcuts. Other electrolytes such as $\text{Na}_2\text{Cr}_2\text{O}_7$, NaNO_3 , and NaClO_3 at 50–250 g/L have also been used, but the choice is limited primarily by cost.

The electrolyte is usually recirculated with the metal products removed or reduced before being reused. This minimizes cost and pollution and prevents the formation of a precipitate in the electrolysis gap.

The effect of electrolyte on surface roughness, H , was studied by Y. Sugie (1978) for five different iron alloys (characterized in Table 9.3) and is shown in Fig. 9.3. The roughness depends on electrolyte and alloy.

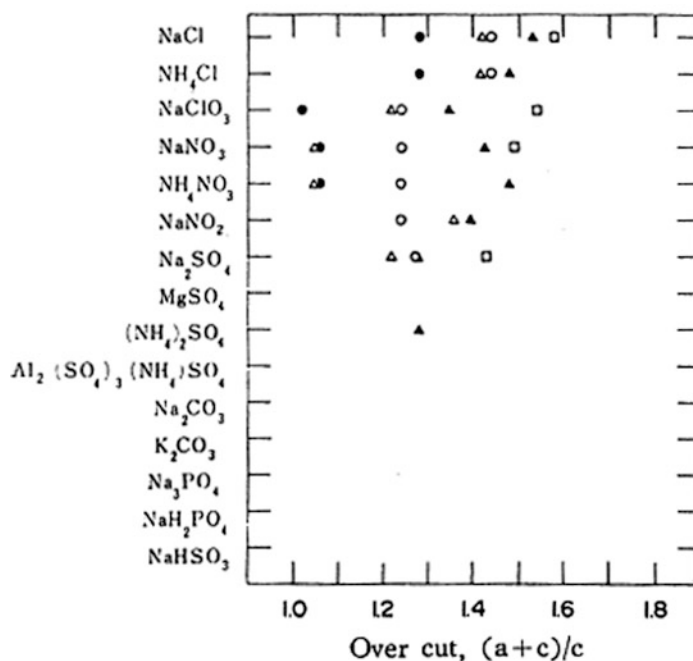


Fig. 9.4 Overcut obtained for various steels (see Table 9.3) in various electrolytes. O SCM 3, ● SKD 11, Δ SNC 2, ▲ SUS 304, □ Inconel 718

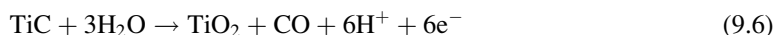
The accuracy of the machining, Figs. 9.4 and 9.5, was determined for the five alloys by measuring the overcut and machined angle (shown in Fig. 9.6) for the various electrolytes. Based on the results, it was concluded that NaClO_3 was most suitable for the low alloy steel and that Na_2SO_4 was best for the high nickel alloy steels.

The power supply and tool drive complete the apparatus. Current densities of $100\text{--}200 \text{ A/cm}^2$ at voltages from 10 to 50 V give cutting rates of about 1 mm/min with surface finishes of $5 \times 10^{-4} \text{ cm}$. By pulsing the DC current, it is possible to reduce the required flow rate of the electrolyte. However, one difficulty, sparking, common in some continuous systems, occurs in intermittent electrolysis and is a decided disadvantage. Other disadvantages in ECM include high initial cost of the equipment, the hazards of hydrogen evolution at the cathode, sparking and “wild cutting” by stray current, and the need of a machinist who has some knowledge of chemistry.

Intergranular corrosion observed for some alloys can be reduced by using mixed electrolytes such as 15% NaCl with 20% NaClO_3 .

It is possible to affect electrochemical grinding and polishing by using a cathodic wheel with an anodic workpiece separated by a flowing electrolyte. Tungsten carbide tools are usually prepared by such a process. An electrochemical saw has also been produced.

Other refractor materials such as TiC, ZrC, TiB_2 , ZrB_2 , TiC/Ni can also be subject to ECM using NaCl and KNO_3 as electrolytes. However, the number of equiv./mol (Z) is usually not a whole number because of multiple dissolution reactions, for example, $Z = 6.6$ for TiC because



as well as



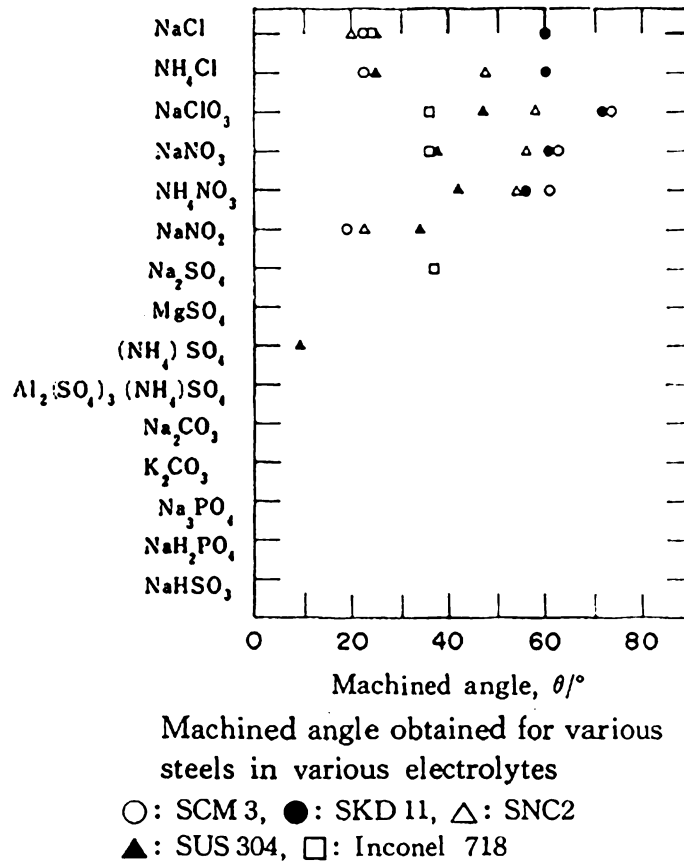


Fig. 9.5 Machined angle obtained for various steels (see Table 9.3) in various electrolytes. ○ SCM 3, ● SKD 11, △ SNC 2, ▲ SUS 304, □ Inconel 718

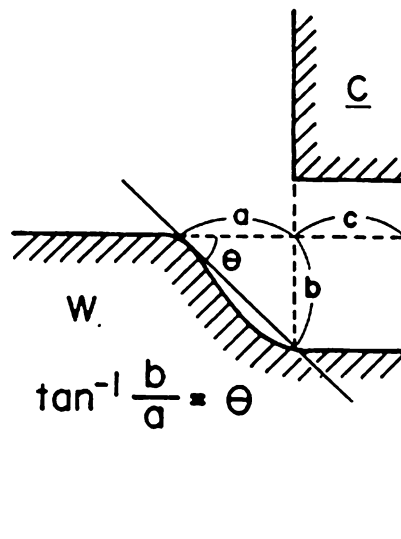


Fig. 9.6 Schematic diagram of machined surface (see Figs. 9.3, 9.4, and 9.5). W working electrode (15 mmφ), C counter electrode (5 mmφ), θ machined angle

One interesting result of ECM is that the surface composition of an alloy may be significantly different from the bulk composition. Thus, a TiC/Ni alloy of Ni, Ti, C, O of 11, 44, 39, and 6 at.%, respectively, had a surface composition of 47, 22, 10, and 21 at.% after ECM. This difference disappears within 1 μm from the surface and reflects the preferential dissolution of one or more elements in the metal.

The major disadvantages of ECM over conventional machining are the high cost of the ECM machine and its high maintenance cost, the technical expertise required of the operator, and the lower accuracy achieved.

9.5 Electrodeics

A metal in equilibrium with its ions in solution will establish a potential difference which depends on the concentration of the metal ion in solution and the temperature. This potential is best determined by comparison with a standard which is arbitrarily set to zero—the hydrogen electrode:



The electrical energy, \mathcal{E} , is directly related to the free energy, ΔG , by the relation

$$\Delta G = -n\mathcal{F}\mathcal{E} \quad (9.9)$$

where n is the number of electrons transferred in the process and \mathcal{F} is the Faraday. For an equilibrium reaction,

$$\Delta G = \Delta G^\circ + RT \ln Q \quad (9.10)$$

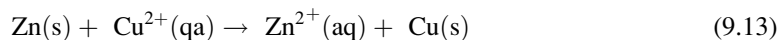
where ΔG° is the standard free energy and

$$\Delta G^\circ = -RT \ln K_{\text{eq}} \quad (9.11)$$

R is the gas constant equal to 8.314 J/K.mol; T is the absolute temperature; Q is the ratio of the concentration of products to concentration of reactants, and K_{eq} is the value of the equilibrium constant at the specified temperature. For a chemical reaction, (9.9) becomes

$$\mathcal{E} = \mathcal{E}^\circ - RT \ln Q \quad (9.12)$$

which is called the Nernst equation. For example, in the Daniell cell,



$$\mathcal{E} = \mathcal{E}^\circ - \frac{RT}{n\mathcal{F}} \ln \frac{[\text{Zn}^{2+}]}{[\text{Cu}^{2+}]} \quad (9.14)$$

Reaction (9.13) can be considered to be composed of two reactions called *half-cell* reactions:



and



Table 9.4 Standard reduction potentials for some common redox systems at 25°C (↑ signifies gas state, and ↓ represents solid state; in all other cases, state is liquid or solution)

Reduction half-reaction	$\mathcal{E}^{\circ}_{cell}(\text{V})$	Reduction half-reaction	$\mathcal{E}^{\circ}_{cell}(\text{V})$
$\text{F}_2 \uparrow + 2\text{e}^- = 2\text{F}^-$	+2.87	$\text{Cu}^+ + \text{e}^- = \text{Cu} \downarrow$	+0.521
$\text{O}_3 \uparrow + 2\text{H}^+ + 2\text{e}^- = \text{O}_2 \uparrow + \text{H}_2\text{O}$	+2.07	$\text{Fe}(\text{CN})_6^{3-} + \text{e}^- = \text{Fe}(\text{CN})_6^{4-}$	+0.356
$\text{Co}^{3+} + \text{e}^- = \text{Co}^{2+}$	+1.82	$\text{Cu}^{2+} + 2\text{e}^- = \text{Cu} \downarrow$	+0.337
$\text{H}_2\text{O}_2 + 2\text{H}^+ + 2\text{e}^- = 2\text{H}_2\text{O}$	+1.77	$\text{Hg}_2\text{Cl}_2 \downarrow + 2\text{e}^- = 2\text{Hg} + 2\text{Cl}^-$	+0.2680
$\text{Ce}^{4+} + \text{e}^- = \text{Ce}^{3+}(\text{in HClO}_4 \text{ solution})$	+1.70	$\text{AgCl} \downarrow + \text{e}^- = \text{Ag} \downarrow + \text{Cl}^-$	+0.2224
$\text{MnO}_4^- + 4\text{H}^+ + 3\text{e}^- = \text{MnO}_2 \downarrow + 2\text{H}_2\text{O}$	+1.69	$\text{Cu}^{2+} + \text{e}^- = \text{Cu}^+$	+0.153
$2\text{HClO} + 2\text{H}^+ + 2\text{e}^- = \text{Cl}_2 \uparrow + 2\text{H}_2\text{O}$	+1.63	$\text{Sn}^{4+} + 2\text{e}^- = \text{Sn}^{2+}(\text{in HCl solution})$	+0.14
$\text{Ce}^{4+} + \text{e}^- = \text{Ce}^{3+}(\text{in HNO}_3 \text{ solution})$	+1.60	$\text{S} \downarrow + 2\text{H}^+ + 2\text{e}^- = \text{H}_2\text{S}$	+0.14
$2\text{HBrO} + 2\text{H}^+ + 2\text{e}^- = \text{Br}_2 + 2\text{H}_2\text{O}$	+1.6	$\text{S}_4\text{O}_6^{2-} + 2\text{e}^- = 2\text{S}_2\text{O}_3^{2-}$	+0.09
$\text{MnO}_4^- + 8\text{H}^+ + 5\text{e}^- = \text{Mn}^{2+} + 4\text{H}_2\text{O}$	+1.51	$2\text{H}^+ + 2\text{e}^- = \text{H}_2 \uparrow$	0.0000
$2\text{BrO}_3^- + 12\text{H}^+ + 10\text{e}^- = \text{Br}_2 + 6\text{H}_2\text{O}$	+1.5	$\text{Pb}^{2+} + 2\text{e}^- = \text{Pb} \downarrow$	-0.126
$\text{Mn}^{3+} + \text{e}^- = \text{Mn}^{2+}$	+1.49	$\text{Sn}^{2+} + 2\text{e}^- = \text{Sn} \downarrow$	-0.140
$\text{Ce}^{4+} + \text{e}^- = \text{Ce}^{3+}(\text{in H}_2\text{SO}_4 \text{ solution})$	+1.44	$\text{Ni}^{2+} + 2\text{e}^- = \text{Ni} \downarrow$	-0.23
$\text{Cl}_2 \uparrow + 2\text{e}^- = 2\text{Cl}^-$	+1.359	$\text{Co}^{2+} + 2\text{e}^- = \text{Co} \downarrow$	-0.28
$\text{Cr}_2\text{O}_7^{2-} + 14\text{H}^+ + 6\text{e}^- = 2\text{Cr}^{3+} + 7\text{H}_2\text{O}$	+1.33	$\text{Cr}^{3+} + \text{e}^- = \text{Cr}^{2+}(\text{in HCl solution})$	-0.38
$\text{Ce}^{4+} + \text{e}^- = \text{Ce}^{3+}(\text{in HCl solution})$	+1.28	$\text{Cd}^{3+} + 2\text{e}^- = \text{Cd} \downarrow$	-0.402
$\text{MnO}_2 \downarrow + 4\text{H}^+ + 2\text{e}^- = \text{Mn}^{2+} + 2\text{H}_2\text{O}$	+1.23	$\text{Fe}^{2+} + 2\text{e}^- = \text{Fe} \downarrow$	-0.440
$\text{O}_2 \uparrow + 4\text{H}^+ + 2\text{e}^- = 2\text{H}_2\text{O}$	+1.229	$2\text{CO}_2 \uparrow + 2\text{H}^+ + 2\text{e}^- = \text{H}_2\text{C}_2\text{O}_4$	-0.49
$\text{ClO}_4^- + 2\text{H}^+ + 2\text{e}^- = \text{ClO}_3^- + \text{H}_2\text{O}$	+1.19	$\text{Cr}^{3+} + 3\text{e}^- = \text{Cr} \downarrow$	-0.74
$2\text{IO}_3^- + 12\text{H}^+ + 10\text{e}^- = \text{I}_2 \downarrow + 6\text{H}_2\text{O}$	+1.19	$\text{Zn}^{2+} + 2\text{e}^- = \text{Zn} \downarrow$	-0.7628
$\text{Br}_2 + 2\text{e}^- = 2\text{Br}^-$	+1.087	$\text{SO}_4^{2-} + \text{H}_2\text{O} + 2\text{e}^- = \text{SO}_3^{2-} + 2\text{OH}^+$	-0.93
$\text{N}_2\text{O}_4 \uparrow + 2\text{H}^+ + 2\text{e}^- = 2\text{HNO}_2$	+1.07	$\text{Mn}^{2+} + 2\text{e}^- = \text{Mn} \downarrow$	-1.190
$\text{NO}_3^- + 3\text{H}^+ + 2\text{e}^- = \text{HNO}_2 + \text{H}_2\text{O}$	+0.94	$\text{Al}^{3+} + 3\text{e}^- = \text{Al} \downarrow$	-1.66
$2\text{Hg}^{2+} + 2\text{e}^- = \text{Hg}_2^{2+}$	+0.907	$\text{H}_2 \uparrow + 2\text{e}^- = 2\text{H}^-$	-2.25
$2\text{NO}_3^- + 4\text{H}^+ + 2\text{e}^- = \text{N}_2\text{O}_4 \uparrow + 2\text{H}_2\text{O}$	+0.80	$\text{Mg}^{2+} + 2\text{e}^- = \text{Mg} \downarrow$	-2.37
$\text{Ag}^+ + \text{e}^- = \text{Ag} \downarrow$	+0.7994	$\text{Na}^+ + \text{e}^- = \text{Na} \downarrow$	-2.7
$\text{Hg}_2^{2+} + 2\text{e}^- = 2\text{Hg}$	+0.792	$\text{Ca}^{2+} + 2\text{e}^- = \text{Ca} \downarrow$	-2.87
$\text{Fe}^{3+} + \text{e}^- = \text{Fe}^{2+}$	+0.771	$\text{Sr}^{1+} + 2\text{e}^- = \text{Sr} \downarrow$	-2.89
$\text{O}_2 \uparrow + 2\text{H}^+ + 2\text{e}^- = \text{H}_2\text{O}_2$	+0.69	$\text{Ba}^{2+} + 2\text{e}^- = \text{Ba} \downarrow$	-2.90
$\text{H}_3\text{AsO}_4 + 2\text{H}^+ + 2\text{e}^- = \text{HAsO}_2 + 2\text{H}_2\text{O}$	+0.56	$\text{K}^+ + \text{e}^- = \text{K} \downarrow$	-2.925
$\text{I}_3^- + 2\text{e}^- = 3\text{I}^-$	+0.545	$\text{Rb}^+ + \text{e}^- = \text{Rb} \downarrow$	-2.93
$\text{I}_2 + 2\text{e}^- = 2\text{I}^-$	+0.536	$\text{Li}^+ + \text{e}^- = \text{Li} \downarrow$	-3.03

The potential of these half-cell reactions can be determined by comparison with the hydrogen electrode² all under standard conditions, which is unit concentration for ions in solution and 1 atm pressure for gases at 25°C. The value of these standard electrode reduction potentials is given in Table 9.4. The standard cell potential of reaction (9.15) is

$$\mathcal{E}^{\circ}\text{Zn}/\text{Zn}^{2+} = -\mathcal{E}^{\circ}\text{Zn}^{2+}/\text{Zn} = 0.763 \text{ V}, \quad \mathcal{E}^{\circ}\text{Cu}^{2+}/\text{Cu} = 0.337 \text{ V}$$

and

$$\mathcal{E}^{\circ}_{cell} = 0.763 + 0.337 = 1.100 \text{ V}$$

² The standard potential of the hydrogen electrode (SHE) is defined as zero at all temperatures for $[\text{H}^+]_{\text{aq}} = 1 \text{ M}$ and $P(\text{H}_2) = 1 \text{ atm}$.

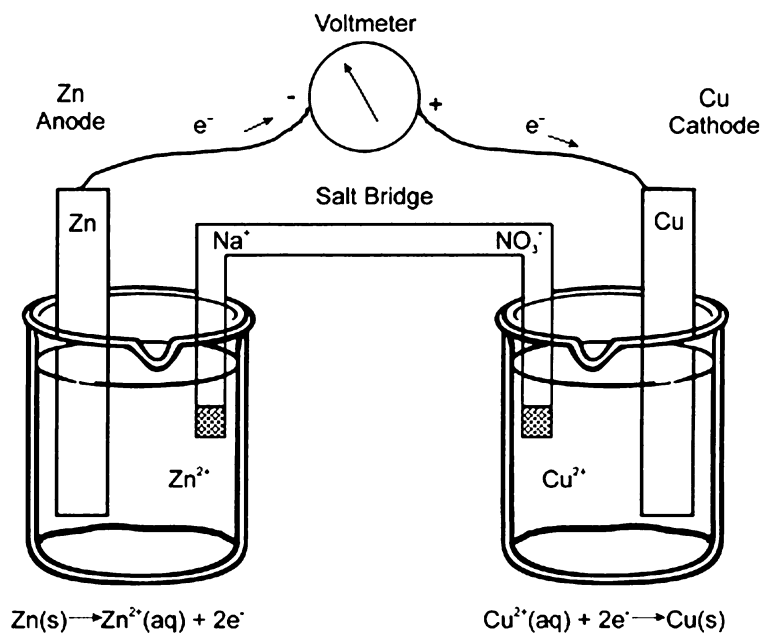


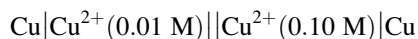
Fig. 9.7 The zinc–copper Daniell cell where the zinc dissolves at the anode (–) and copper is plated out at the cathode (+)

This is represented in shorthand notation as



where the single | line indicates a phase change and the double || line represents a salt bridge or connection between the two half-cells. This is illustrated in Fig. 9.7.

The simplest cell is one in which the electrode material is the same in each half-cell, but the metal ion concentration is different in the two half-cells. This is called a *concentration cell*, an example of such a cell is



The cell potential is

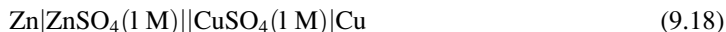
$$\mathcal{E}_{\text{cell}} = \mathcal{E}_{\text{cell}}^{\circ} - \frac{RT}{nF} \ln \frac{0.01}{0.10}, \quad \mathcal{E}_{\text{cell}} = 0 - \frac{0.2568}{2} \ln 0.10, \quad \mathcal{E}_{\text{cell}} = 0.0296\text{ V}$$

The cell will continue to develop a potential until the concentration of Cu^{2+} in the two half-cells becomes equal.

The concentration inequality adjacent to metals is the basis of the corrosion of metals which is discussed in the next chapter. All redox reactions can be divided into two or more half-cells which can be combined into a full-cell. The voltage generated and the current which can be drawn determine its usefulness as a battery.

9.6 Batteries and Cells

The means by which chemical energy is stored and converted into electrical energy is called a *battery* or *cell*. We saw how the Daniell cell composed of a zinc electrode immersed in a 1 M zinc sulfate solution and a copper electrode dipping into a 1 M copper sulfate



will develop 1.10 V.

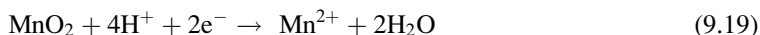
This cell, however, has limited use because as soon as current is drawn from the cell, the voltage drops because of polarization which is primarily caused by the buildup of hydrogen at the copper electrode. This polarization can be minimized by the addition of a depolarizer which supplies oxygen readily and so removes the hydrogen from the electrode to form water. Such a cell, nonetheless, has a limited lifetime and restricted use.

Batteries are classified as primary or secondary. Batteries which are not rechargeable are referred to as primary batteries. Secondary batteries are rechargeable either by an electrical current or by a replacement of the electrode material (anode).

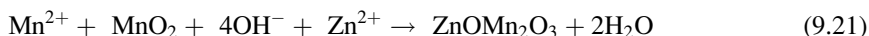
9.6.1 Primary Batteries

A dry cell, which has become a primary power source for transistorized electronic equipment, was developed over a hundred years ago in 1865, is called the *Leclanché* cell.

It consists of a zinc negative electrode, which acts as the container and which is slowly oxidized; a porous carbon rod as the positive electrode, which takes no part in the overall reaction but can act as a gas vent for the cell; and an electrolyte, which is ammonium chloride to which is added manganese dioxide. The MnO_2 acts as a depolarizer and is reduced at the carbon electrode by the following reaction:



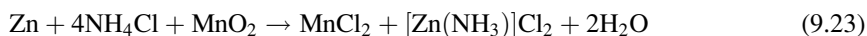
This is complicated by further reactions:



The zinc ion is then complexed by the ammonia as follows:



The cell voltage is between 1.5 and 1.6 V. A D-type battery, commonly used in flashlights, has a capacity of about 4 amp-h. Although this type of cell contains about 20 g of zinc, only about 5 g is used. The overall reaction, although complex, can be represented as follows:



Because the reduction reaction of MnO_2 is not a well-defined reaction, the Nernst equation cannot be applied successfully, and the cell voltage changes unpredictably with time and discharge condition.

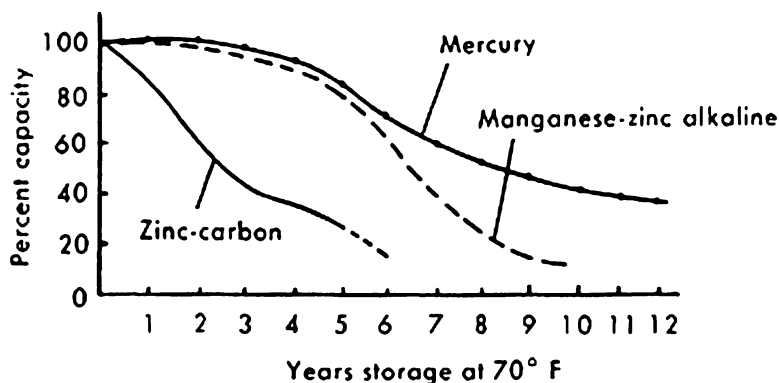
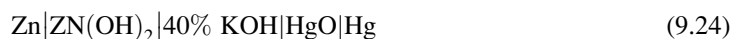


Fig. 9.8 Plots showing the loss in capacity with storage time for the zinc-carbon, manganese-zinc-alkaline, and mercury batteries

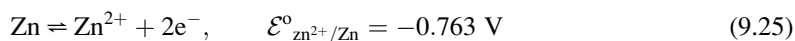
The shelf life of this battery is rather poor, as shown in Fig. 9.8, because of the slow loss of water and because of side reactions due to impurities in the MnO_2 ore commonly used. When specially purified MnO_2 is used, the performance of the battery is greatly improved. The zinc-carbon dry cell is considered the workhorse of the battery industry: It provides power at a very low cost.

Another popular dry cell that is commonly associated with transistorized electronic components is the manganese-zinc alkaline cell. It utilizes refined MnO_2 , as does the improved zinc-carbon cell, but in large excess. The electrolyte is 40% KOH presaturated with zinc (ZnO) to prevent the zinc electrode from dissolving while in storage. A steel can, instead of the zinc electrode, usually serve as the container; hence, the cell is highly leak resistant. However, the cost of the cell is about twice that of the zinc-carbon cell.

The most efficient dry cell is the mercury cell, which has an excellent stabilized voltage. Developed in 1942 by Ruben, it consists of zinc, which dissolves and becomes the negative electrode and mercuric oxide, which is reduced to mercury at the positive electrode. The overall cell, which has no salt bridge, can be represented as follows:



One half-cell reaction is

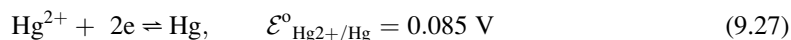


This is followed by the reaction

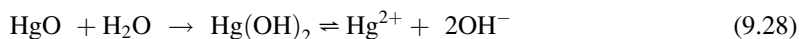


for which $K_{\text{sp}} = 4.5 \times 10^{-17}$.

The other half-cell reaction is



This is preceded by the reaction



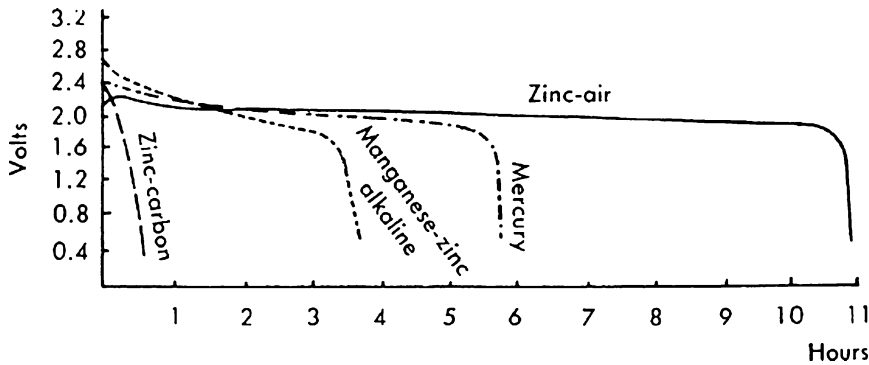


Fig. 9.9 Typical discharge curves of voltage plotted against time for four different types of cells of comparable size (two AA penlight cells discharged at 250 mA)

for which $K_{sn} = 1.7 \times 10^{-26}$. The cell emf is given as follows:

$$\begin{aligned}\mathcal{E}_{\text{cell}} &= \mathcal{E}_{\text{Zn/Zn}^{2+}} + \mathcal{E}_{\text{Hg}^{2+}/\text{Hg}} = -(\mathcal{E}_{\text{Zn}^{2+}/\text{Zn}}) + \mathcal{E}_{\text{Hg}^{2+}/\text{Hg}} \\ \mathcal{E}_{\text{cell}} &= -\left(\mathcal{E}_{\text{Zn}}^{\circ} - \frac{RT}{n\mathcal{F}} \ln \frac{1}{[\text{Zn}^{2+}]}\right) + \left(\mathcal{E}_{\text{Hg}}^{\circ} - \frac{RT}{n\mathcal{F}} \ln \frac{1}{[\text{Hg}^{2+}]}\right)\end{aligned}\quad (9.29)$$

However,

$$[\text{Zn}^{2+}] = \frac{K_{\text{sp}}(\text{Zn}(\text{OH})_2)}{[\text{OH}^-]_2} \quad \text{and} \quad [\text{Hg}^{2+}] = \frac{K_{\text{sp}}(\text{Hg}(\text{OH})_2)}{[\text{OH}^-]_2} \quad (9.30)$$

$$\begin{aligned}\mathcal{E}_{\text{cell}} &= -\left(\mathcal{E}_{\text{Zn}}^{\circ} - \frac{0.02568}{2} \ln \frac{[\text{OH}^-]^2}{K_{\text{sp}}(\text{Zn}(\text{OH})_2)}\right) + \left(\mathcal{E}_{\text{Hg}}^{\circ} - \frac{0.02568}{2} \ln \frac{[\text{OH}^-]^2}{K_{\text{sp}}(\text{Hg}(\text{OH})_2)}\right) \\ &= -\mathcal{E}_{\text{Zn}}^{\circ} + \mathcal{E}_{\text{Hg}}^{\circ} + \frac{0.02568}{2} \ln \frac{K_{\text{sp}}(\text{Hg}(\text{OH})_2)}{K_{\text{sp}}(\text{Zn}(\text{OH})_2)} \\ &= 0.763 + 0.850 + \frac{0.02568}{2} \ln \frac{1.7 \times 10^{-26}}{4.5 \times 10^{-17}} \\ &= 1.613 + \frac{0.02568}{2} \ln 3.8 \times 10^{-10} \\ \mathcal{E}_{\text{cell}} &= 1.613 - 0.278 = 1.335 \text{ V}\end{aligned}$$

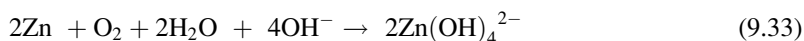
This value compares favorably with the actual cell voltage of about 1.35 V. Thus, the cell potential is independent of the concentration of the electrolyte, $[\text{OH}^-]$. The cell has a low internal resistance and has a very long shelf life when compared to the other two dry cells discussed previously, as shown in Fig. 9.8. For example, after a 3-year storage, a typical cell voltage changed from an initial value of 1.357 to 1.344 V; that is, there was about a 1% change. Thus, the use of the mercury dry cell as a reference voltage is widespread. A comparison of cell voltage of the three types of dry cells with time during constant current drain is shown in Fig. 9.9. The remarkable constancy in voltage of the mercury cell in contrast to the sharp voltage drop in the zinc-carbon and manganese-zinc alkaline cells is obvious. The mercury cell, although initially about three times more expensive than the

zinc–carbon cell, has a lower operating cost per hour than either of the other two dry cells. Therefore, it is not too difficult to understand why the mercury cell is being used increasingly as a convenient source of power and reference voltage.

Also shown in Fig. 9.9 is the voltage curve for the zinc–air cell. The cell consists of an anode of amalgamated zinc powder in contact with the electrolyte, which is concentrated potassium hydroxide, and a cathode of metal mesh, which is a catalyst for the conversion of oxygen to the hydroxide ion. The half-reactions are

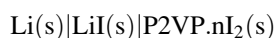


and the overall reaction is



The cell is encased in a porous polymer that allows oxygen from the air to diffuse to the cathode but does not allow the electrolyte to leak out. The shelf life is almost indefinite when the cell is stored in an airtight container. The cell is used to best advantage when continuous high currents are required for a short period of time, since it cannot be left in contact with air without losing capacity. Resealing the cell or cutting off the air supply to the cell when it is not in use extends the life during intermittent use. The catalytic cathode for the zinc–air cell is a direct development from work on fuel cells, which are discussed later.

In contrast to the zinc–air battery, the lithium–iodine solid LiI electrolyte battery will last for almost 15 years. A 120-mAh battery with an initial voltage of 2.8 V drops to 2.6 V when discharged continuously at about 1 μA . The cell is written as



where P2VP.nI₂ is a complex between poly-2-vinylpyridine (P2VP) and iodine. The reaction is given as



This type of cell is highly reliable, and it is commonly used in cardiac pacemaker batteries which are implanted.

The temperature coefficient of a cell's potential is determined by the change in free energy, ΔG , with temperature and is given by

$$\frac{d\varepsilon^\circ}{dT} = \frac{\Delta S^\circ}{n\mathcal{F}} \quad (9.35)$$

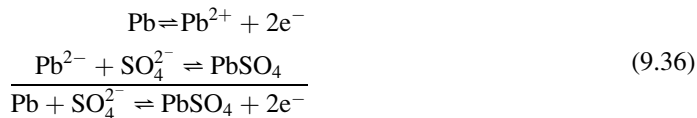
where ΔS° is the standard entropy change for the reaction.

9.6.2 Secondary Batteries

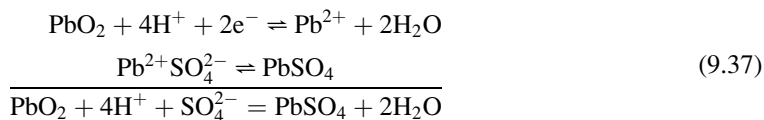
The most common secondary battery is the lead storage battery, which has as an essential feature and ability to be recharged. The cell consists of a lead plate for the negative electrode, separated by a

porous spacer from the positive electrode, which is composed of porous lead dioxide. The electrolyte is sulfuric acid—about 32% by weight. The electrode reactions are as follows:

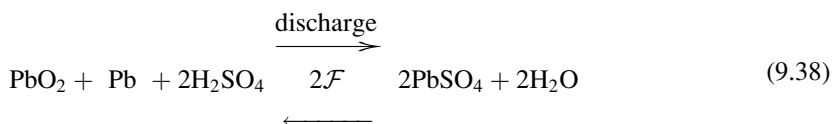
Negative electrode



Positive electrode



The net overall reaction is as follows:



Polarization by hydrogen is minimized by the PbO_2 electrode, which is also a depolarizer. The discharge of the battery consumes acid and forms insoluble lead sulfate and water; that is, the density of the solution decreases from about 1.28 g/cm^3 in the fully charged condition to about 1.1 g/cm^3 in the discharged state. The overall open cell voltage (when no current is being drawn) depends on the acid concentration (i.e., SO_4^{2-} ion concentration, which in turn controls the concentration of the Pb^{2+} ion via the K_{sp} for PbSO_4). The voltage varies from 1.88 V at 5% H_2SO_4 by weight to 2.15 V at 40% acid by weight. The conductivity of aqueous H_2SO_4 is at a maximum when H_2SO_4 is about 31.4% by weight at 30°C (or 27% at -20°C); it is best to control concentration in this range since the internal resistance of the battery is at a minimum. Another factor influencing the choice of the acid concentration is the freezing point of the sulfuric acid solution; thus, in cold climates, a higher acid level (38% H_2SO_4 by weight, specific gravity 1.28) is required in order to minimize the possibility of the electrolyte freezing at the relatively common temperature of -40°C . The amount of lead and lead dioxide incorporated into the electrodes is three to four times the amount used in the discharging process because of the construction of the electrodes and the need for a conducting system that makes possible the recharging of a “dead” battery.

In 1988, a collection of 8,256 lead–acid batteries was used by a California electric power plant to store energy and to deliver it during peak power demands, that is, load leveling. The batteries contained over 1,800 tonnes of lead and could supply 10 MWe for 4 h, enough to meet the electrical demands of 4,000 homes. The efficiency of the system was rated at 75%.

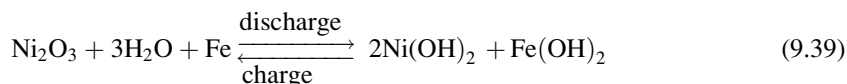
The capacity of a battery is rated in terms of amp-hours and depends on the rate of discharge and, even more significantly, on the temperature. For example, a battery with a rating of 90 amp-h at 25°C has a rating of about 45 amp-h at -12°C and about 36 amp-h at -18°C . The lead–acid battery in the fully discharged state slowly loses capacity since the lead sulfate recrystallizes, and some of the larger crystals are then not available for the reverse charge reaction. When this happens, the battery is said to be sulfonated. This can be remedied by the process of removing the “insoluble” sulfate, recharging the battery, and reconstituting the acid to the appropriate specific gravity.

In respect to this property as well as others, the nickel–alkaline battery is superior to—although about three times more costly than—the lead–acid battery. There are two types of nickel–alkaline storage batteries: the Edison nickel–iron battery and the nickel–cadmium battery.

In the Edison battery, the cell can be represented as follows:

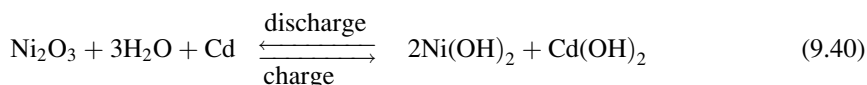


The overall reaction is as follows:



The cell potential has an average value of 1.25 V. Although the overall reaction does not apparently involve the electrolyte, the KOH does in fact participate in each of the half-cell reactions. Although the Edison battery is designed and suitable for regular cyclic service, the efficiency of charge is only 60%; thus, it has now been almost completely replaced by the more efficient (72%) nickel–cadmium battery, which is itself inferior in energy efficiency to the lead–acid battery with an efficiency of about 80%.

In the nickel–cadmium alkaline storage battery, the iron of the Edison cell is replaced by cadmium to give the following equivalent reaction:



The average cell voltage of 1.2 V is slightly lower than that of the Edison cell. Cadmium is preferred to iron in the nickel–alkaline cell because cadmium hydroxide is more conductive than iron hydroxide. The absence of higher oxidation states for cadmium minimizes side reactions, which occur in the Edison cell. The nickel–cadmium cell can also be charged at a lower voltage since there is no overvoltage, as there is at the iron electrode.

One major disadvantage of the nickel–alkaline battery is the alkaline electrolyte, which picks up CO_2 from the atmosphere and must therefore be replaced periodically. However, the advantages of the nickel–cadmium cell over the lead–acid battery are numerous; some of these are as follows:

1. The freezing point of the KOH electrolyte is low (about -30°C) regardless of the state of charge.
2. The capacity does not drop as sharply with drop in temperature.
3. The cell can be charged and discharged more often and at higher rates (without gassing) and thus has a longer useful life.

The storage battery has become an accepted source of power in our modern technological world, and in an environment-conscious society, the storage battery will play an ever increasing role.

Table 9.5 Values of standard cell voltages of selected fuel cell reactions at 25°C

Reaction	$\mathcal{E}_{\text{cell}}^{\circ}$ (V)
$2\text{C} + \text{O}_2 \rightarrow 2\text{CO}$	0.70
$\text{C} + \text{O}_2 \rightarrow \text{CO}_2$	1.02
$\text{CH}_4 + 2\text{O}_2 \rightarrow \text{CO}_2 + 2\text{H}_2\text{O}$	1.04
$\text{C}_3\text{H}_8 + 5\text{O}_2 \rightarrow 3\text{CO}_2 + 4\text{H}_2\text{O}$	1.10
$4\text{NH}_3 + 3\text{O}_2 \rightarrow 2\text{N}_2 + 6\text{H}_2\text{O}$	1.13
$\text{CH}_3\text{OH} + \frac{3}{2}\text{O}_2 \rightarrow \text{CO}_2 + 2\text{H}_2\text{O}$	1.21
$\text{H}_2 + \frac{1}{2}\text{O}_2 \rightarrow \text{H}_2\text{O}(\text{l})$	1.23
$2\text{CO} + \text{O}_2 \rightarrow 2\text{CO}_2$	1.33
$\text{N}_2\text{H}_4 + \text{O}_2 \rightarrow \text{N}_2 + 2\text{H}_2\text{O}$	1.56
$2\text{Na} + \text{H}_2\text{O} + \frac{1}{2}\text{O}_2 \rightarrow 2\text{NaOH}$	3.14

9.7 Fuel Cells

The discovery of the fuel cell followed soon after Faraday developed his laws of electrolysis. In 1839, Grove showed that the electrolysis of water was partially reversible. Hydrogen and oxygen formed by the electrolysis of water were allowed to recombine at the platinum electrodes to produce a current or what appeared to be “reverse electrolysis.” Using the same fundamental principles but somewhat more advanced technology, Bacon in 1959—after about 20 years of intensive effort—produced a 6 kW power unit that could drive a small truck.

It was recognized early that the overall thermodynamic efficiency of steam engines is only about 15%. The efficiency of modern electrical generators is about 20–50%, whereas the efficiency of the fuel cell (in which there is direct conversion of chemical energy into electrical energy) does not have any thermodynamic limitation. Theoretically, the efficiency of the fuel cell can approach 100%, and in practice, efficiency of over 80% can be achieved.

Interest in the fuel cell has increased remarkably in the last decade primarily because of (1) the high efficiency associated with the energy conversion, (2) the low weight requirement essential for satellite and spacecraft power sources that is readily satisfied with hydrogen as a fuel, and (3) the recent requirement of a pollution-free power source.

Any redox system with a continuous supply of reagents is potentially a fuel cell. Some reactions that have been studied are given in Table 9.5 with the corresponding theoretical $\mathcal{E}_{\text{cell}}^{\circ}$ values, which are calculated from thermodynamic data ($\Delta G^{\circ} = -n\mathcal{F}\mathcal{E}^{\circ}$). The temperature coefficients of the $\mathcal{E}_{\text{cell}}^{\circ}$ values of some of the reactions in Table 9.5 are shown in Fig. 9.10.

In practice, the suitability of a reaction system is determined by the kinetics of the reaction, which depends on temperature, pressure of gases, electrode polarization, surface area of electrodes, and presence of a catalyst. A fuel cell that is thermodynamically and kinetically feasible must be considered from an economic viewpoint before it is accepted. Thus, since hydrogen, hydrazine, and methanol are too expensive for general application, their use in fuel cells has been limited to special cases. Hydrogen has been used for fuel cells in satellites and space vehicles, in which reliability and lightness are more important than cost. Hydrazine fuel cells have been used in portable-radio power supplies for the United States Army because of their truly silent operation. Methanol fuel cells have been used to power navigation buoys and remote alpine television repeater stations because such power systems are comparatively free from maintenance problems over periods of a year or more. The polarization at the electrodes of a fuel cell is the most important single factor that limits the usefulness of the cell. The various polarization characteristics for a typical fuel cell are plotted separately as a function of current density in Fig. 9.11.

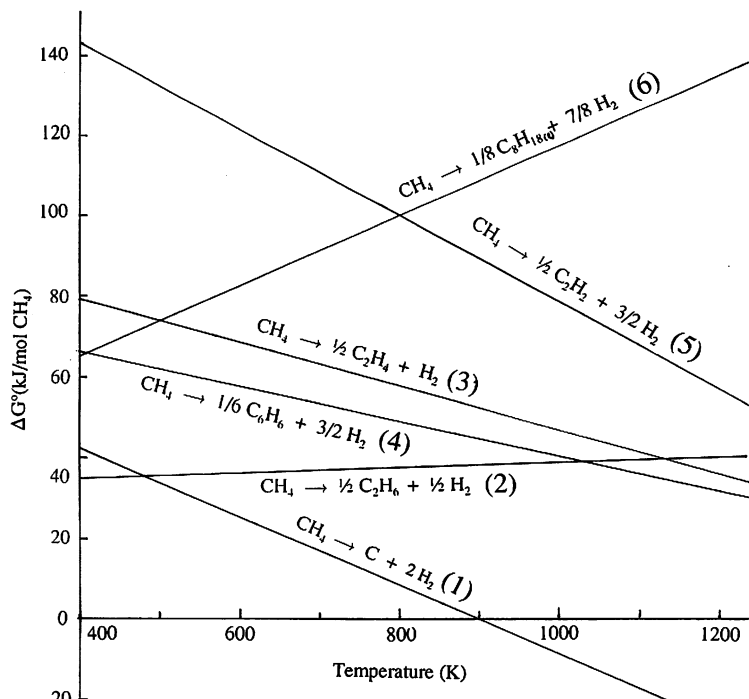


Fig. 9.10 Effect of temperature on the cell voltage, $\mathcal{E}^\circ_{\text{cell}}$, for some fuel cell reactions. *Note:* Slope is related to the entropy change of the reaction

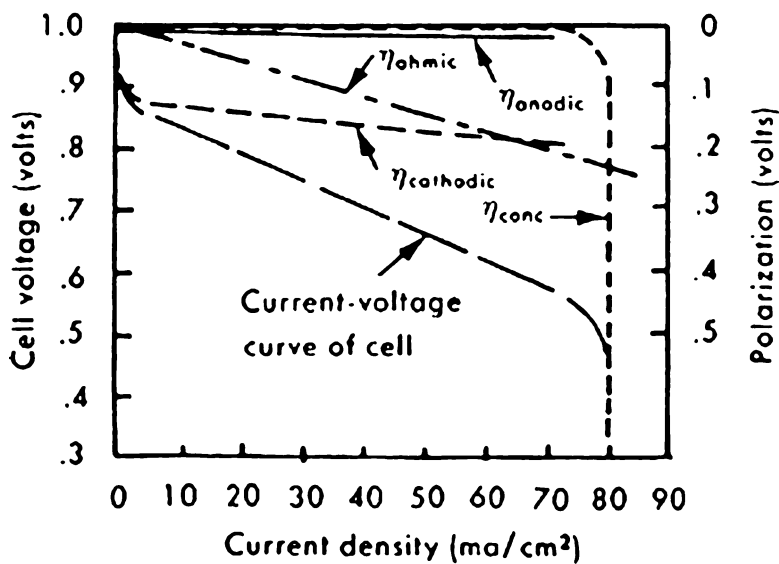


Fig. 9.11 Operating characteristics of a typical fuel cell. Net polarization is given by $\eta_{\text{total}} = \eta_{\text{anodic}} + \eta_{\text{cathodic}} + \eta_{\text{ohmic}} + \eta_{\text{conc}}$

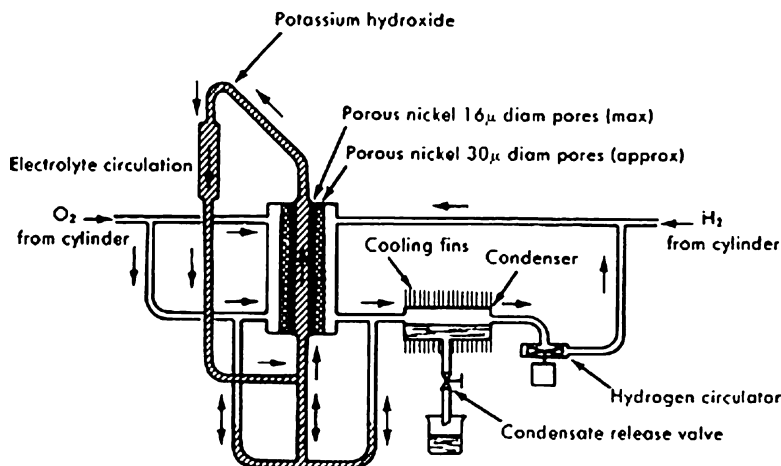
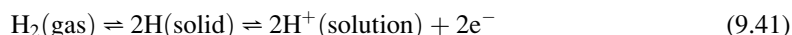
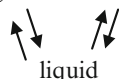


Fig. 9.12 Bacon hydrogen–oxygen fuel cell with gas-diffusion electrodes

The most successful fuel cell to date is the hydrogen–oxygen fuel cell, which deserves special attention since it has been used in the Apollo and Gemini space flights and moon landings. The reaction



occurs at the gas = solid interface.



To facilitate the rapid attainment of equilibrium, a liquid gas-diffusion electrode was developed whereby concentration polarization could be minimized. The ohmic polarization (the RI drop between the electrodes, which gives rise to an internal resistance) is also minimized when the anode-to-cathode separation is reduced. The apparatus of the hydrogen–oxygen fuel cell developed by Bacon with gas-diffusion electrodes is shown in Fig. 9.12. The operating temperature of 240°C is attained with an electrolyte concentration of about 80% KOH solution, which with the high pressures of about 600 psi for H_2 and O_2 , allows high current densities to be drawn with relatively low polarization losses. Units such as these with power of 15 kW have been built and used successfully for long periods.

Today, fuel cells are still in the development stage, and much further work must be done before an efficient economical fuel cell is produced. The oxidation of coal or oil to CO_2 and H_2O has been achieved in a fuel cell; the system uses platinum as a catalyst and an acid electrolyte at high temperature, and thus the cost of materials for the cell construction is very high. The economic fuel cell-powered automobile, although a distinct possibility, is not to be expected in the immediate future.

9.8 Hybrid Cells

The hybrid cell is one which is not rechargeable by simply reversing the voltage. Some of these use oxygen in air as the cathode material



Table 9.6 Some properties of selected metal–air batteries

Battery	Electrolytes	Cell volt (V)	Energy density (Wh/kg)		Peak power (W/kg)	Cycle life	Comments
			Theoretical	Actual			
Lithium–air $2\text{Li} + \frac{1}{2}\text{O}_2 \rightarrow \text{Li}_2\text{O}$	LiOH	2.9	11.148	290		Mechanical	Unlikely to be developed for commercial use. High Li costs
Aluminum–air $2\text{Al} + 3\text{O}_2 + 3\text{Al}_2\text{O}_3$	NaOH	2.71	8.081	440		Mechanical rechargeable	Prototype developed and tested. Good energy density, low cost
Magnesium–air $2\text{Mg} + \text{O}_2 \rightarrow 2\text{MgO}$	NaCl	3.09	6.813			Mechanical rechargeable	No advantage over Al, not being considered seriously at present

and a metal, for example, Al, as the anode material



Such systems are called *metal–air batteries* and are mechanically rechargeable (anode metal is replaced). Such batteries have only recently become practicable due to the developments of the O_2 – electrode in fuel cells. Some characteristics of selected metal–air batteries are given in Table 9.6.

The aluminum–air battery has recently received some attention as a result of work done by the Lawrence Livermore National Laboratory. It was estimated that a 60-cell system with 230 kg of aluminum can power a VW for 5,000 km before requiring mechanical recharging. Periodic refill with water and removal of $\text{Al}(\text{OH})_3$ would be required after 400 km. The conversion of the $\text{Al}(\text{OH})_3$ back to Al at an electrolytic refinery completes the recycling process. In 1986, an Al–air battery producing 1,680 W was shown to power an electric golf cart for 8 h.

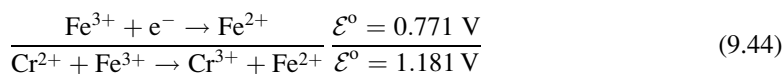
A battery where the active components are flowed past electrodes in a cell with two compartments separated by an appropriate membrane is called a *flow battery*. One such battery is the Fe/Cr redox system

cathode



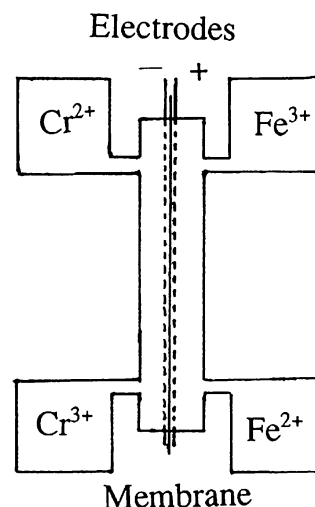
and

anode



The overall voltage is given by

Fig. 9.13 Schematic diagram of a redox cell (battery) using Cr^{2+} and Fe^{3+} aqueous solutions as reactants

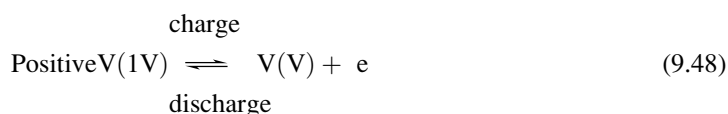
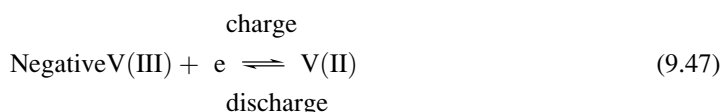


$$\mathcal{E}^0 = \mathcal{E}_{\text{cell}}^0 - 0.059 \log K \quad (9.45)$$

$$\mathcal{E}_{\text{cell}}^0 = 1.181 - 0.059 \log \frac{[\text{Fe}^{2+}][\text{Cr}^{3+}]}{[\text{Fe}^{3+}][\text{Cr}^{2+}]} \quad (9.46)$$

The reactant solutions Cr^{2+} and Fe^{3+} are reacted as shown in Fig. 9.13.

The product solutions are kept separate, and the Fe^{2+} can be oxidized by air back to Fe^{3+} , whereas the Cr^{3+} can be electrolytically reduced back to Cr^{2+} . An Australian redox flow battery has been described which uses vanadium both as oxidant and reductant in the following reactions:



The electrolyte is 2 M VOSO_4 in 2 M H_2SO_4 with graphite plates acting as electrodes to collect the current. The open circuit voltage (OCV) is 1.45 V with a 95% charging efficiency and little or no H_2 or O_2 evolution. One of the major advantages of this battery is that if the membrane leaks, then the separation of the two flow streams is not necessary as in the Fe/Cr system. Several such redox cells are available and being studied primarily as potential power sources for the electric vehicle (EV) which will most assuredly be a reality in the near future.

9.9 Electric Vehicle

The first EV was built in 1839 by Robert Anderson of Aberdeen, Scotland. The first practical one was a taxi introduced in England, 1886, which had 28 bulky batteries and a top speed of 12.8 km/h. By 1904, the electric vehicle was common throughout the world, but its production peaked at about 1910

Table 9.7 A comparison of performance and cost goals for a practical EV battery with those of deep-cycling industrial lead–acid battery

Parameter	Goal	Lead–acid
Cost ~ \$/kWh	45	90
Life (cycles)	1,000	700
Life (years)	10	5
Energy efficiency ($\frac{\text{discharge}}{\text{charge energy}}$)	0.80	0.65
Charge time (h)	1–6	6–8
Discharge time (h)	2–4	2–4
Energy density (Wh/kg)	140	35
Power density—peak (Wh/kg)	200	80
Power density—sustained (Wh/kg)	70	30
Volume density (Wh/L)	200	50
Typical size (kWh)	20–50	20–40

when the self-starting gasoline-powered internal combustion engine began to dominate. This was due to the availability of cheap gasoline and mass-produced cars.

However, the EV is due to make a comeback because of the rising cost of gasoline and diesel fuel, the pollution of the environment, and the prevalence of a second small car in most families. Some of the major American automobile producers have been planning to have an EV on the market for the past 30 years. The major stumbling block is the batteries which must be reliable, lightweight, take hundreds of full discharges and recharges, and be inexpensive as well. The desirable features of an ideal battery are compared in Table 9.7 with the lead–acid battery still used at present in EV. A list of possible batteries and some of their properties are given in Table 9.8. The use of the fuel cell and hybrid fuel cell type power sources must also be included.

The choice of batteries available for an EV is both expanding in number and narrowing in type. Several batteries listed in Table 9.8 are being given commercial pilot production tests. It must be recognized that winter restricts the choice or design of a suitable system for cold-climate regions. Recent tests in Winnipeg, Canada, of a US-made EV using lead–acid batteries showed it to be appropriate in summer (about 80 km/charge), but in winter, the lower capacity resulted in less than 8 km/charge. This could undoubtedly be corrected by an integrated design. Since the batteries are only about 70% efficient on charge, the excess energy (heat) could be stored by insulating the batteries or adding a heat-storing medium such as Glauber's salt (see Chap. 1) between the batteries and the insulation. This, however, adds both weight and volume to the system.

The modern design EV will be lightweight and have minimal aerodynamic drag and rolling resistance, efficient motor control system, and transmission as well as regenerative (battery charging) braking. The usual goal of EV is a range of about 100 km, a maximum speed of 90 km/h, and a cruise speed of 45 km/h, with a recharge time of 8–10 h. It would be interesting to speculate that as the EV becomes common and recharging is performed at night, the resulting power drain may invert the peak load, that is, the greater load would occur overnight. The low vehicle emissions set for California are readily met by the EV, and major automobile manufacturers are striving to meet the demand.

One example is the Mercedes-Benz 5-seater 190 Electro car which develops up to 32 kW (44 hp), has a maximum speed of 115 km/h and an operating range of 150 km. The sodium–nickel chloride batteries were chosen over nickel–cadmium and sodium–sulfur alternatives. The car is shown in Fig. 9.14.

A second example is the use of a hydrogen fuel cell to run a bus. Using a Proton Exchange Membrane Fuel Cell (PEMFC), Ballard of Vancouver has built a prototype bus for Chicago Transit Authority. The bus stores hydrogen at high pressure in cylinders on the roof of the bus—enough to give the bus a 560-km range (see Fig. 9.15). Designs have been developed for a more compact

Table 9.8 Evaluation and characteristics of electric vehicles batteries (values depend on source)

Battery and reaction electrolyte		Temp (°C)	Cell voltage (V)	Energy density		Power peak (W/kg)	Cycle life	Depth charge (%)	Charge efficient (%)	Cost initial \$/ kWh	Projected	Advantage	Disadvantage
				Mass Theoretical (Wh/kg)	Vol. Actual (Wh/L)								
Improved lead-acid ${}^{\text{Pb}}\text{Pb} + \text{PbO}_2 + \text{H}_2\text{SO}_4 \rightarrow 2\text{PbSO}_2 + \text{H}_2\text{O}$	H_2SO_4	0–40	2.05	171/30	30/46	50–100	500	90–60	65	90	50	Now available	Low specific energy marginal peak power limited to about 100 miles (150 km)
Nickel–zinc ${}^{\text{Zn}}\text{Zn} + {}^{\text{Ni}}\text{NiO}(\text{OH}) \rightarrow 2\text{H}_2\text{O} + 2\text{Ni}(\text{OH})_2$	$\text{KOH } 2\text{H}_2\text{O}$	–45+40	1.7	321/66	66/140	150	400	65	65	150	50	Excellent power and volume density. (UK prospect)	Solubility of Zn in KOH shortens shelf life. High Ni cost
Nickel–iron ${}^{\text{Fe}}\text{Fe} + 2\text{NiO}(\text{OH}) + 2\text{H}_2\text{O} \rightarrow \text{Zn}$	KOH	–40+40	1.37	267/55	55/100	75	1,500	90	60	120	65	Developed in 1901 by Edison, now mosure and rugged	Low power density H, garing during charge. Poor peak power at low temperature
Zinc–chlorine ${}^{\text{Zn}}\text{Zn} + \text{Cl}_2 + 6\text{H}_2\text{O} \rightarrow 2\text{NiCl}_2 + 6\text{H}_2\text{O}$	ZnCl_2	<9.0+40	2.12	465/100	100/60	80	400	–	65	100	35	Inexpensive lightweight materials, high power density	Complex system requiring refrigeration and heating, Cl_3 hazard
Sodium–sulfur ${}^{\text{Na}}\text{Na} + \text{YS} \rightarrow \text{Na}, \text{Sy } x = \text{Z}, y = 53$	Al_2O_3	350	1.76–2.08	664/150	150/160	200	300	60	85	50	35	Inexpensive light material, high energy density	Short life due to seals and corrosion, Na hazard. High temperature requirement
Lithium–sulfur ${}^{\text{Li}}\text{Li} + \text{S} \rightarrow \text{Li}_2\text{S}$	LiCl/KC	450	22	2567								Improved with Li/ Al alloy (~5 at. % Li)	Too reactive, Li cost high



Fig. 9.14 Mercedes-Benz zero emission class A EV. The car uses a 40 kW (54 hp)—three-phase induction motor developing a rated torque of 155 Nm which can accelerate the car to 100 km/h in 17 s with a top speed of 120 km/h and a normal usage range of 150 km. Recharging can be made in 6–12 h using normal household sockets. The battery system is sodium/nickel chloride with an energy storage capacity of 100 Wh/kg and a life of over 100,000 km

(volume of 32 L) stack of fuel cells which delivers 32.3 kW and intended for a small passenger vehicle.

General Motors has announced (February 1996) the start of a mass-produced EV powered by lead–acid batteries and which will have a range of about 110 km per charge and a maximum speed of 100 km/h. The estimated cost is expected to be US\$35,000.

It is obvious that much experimental work remains to be done before a reliable and economical EV will be on the market. The incentive—lower fuel costs and a cleaner environment for the EV in comparison to the ICE—will not diminish with time.

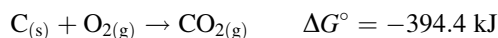
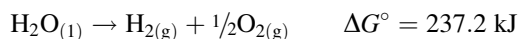
Exercises

1. What is a concentration cell?
2. What is a redox cell?
3. Distinguish between primary and secondary batteries with examples.
4. What factors determine the voltage of a cell and its temperature coefficient?
5. Explain how the capacity of a storage battery is measured.
6. Explain why the capacity of the lead–acid battery drops so rapidly with decrease in temperature.
7. What factors influence the drop in cell voltage of a battery when current is withdrawn?



Fig. 9.15 (a) The Ballard H_2 fuel cell-powered bus and (b) the FirstEnergy fuel cell unit (Ballard Power)

8. The voltage of the H_2 – O_2 fuel cell is given by $\Delta G^\circ = -n\mathcal{F}\mathcal{E}^\circ$ where n is the number of electrons transferred in the reaction, \mathcal{F} is the Faraday, and ΔG is the standard free energy change in the reaction. Show that $\mathcal{E}^\circ = 1.23$ V from thermodynamic data.
9. Explain why in the electrolysis of water into H_2 and O_2 , the voltage required is greater than 1.23 V.
10. (a) Calculate the voltage of the methanol–oxygen fuel cell.
 (b) Explain why the voltage will be lower if air was used instead of pure oxygen.
 (c) Calculate the standard voltage for the methanol–air fuel cell.
11. The approximate energy consumption for an EV is 0.16 kWh/km to 0.32 kWh/mile. If electrical energy is priced at 3 ¢/kWh, calculate the energy cost/km for an EV.
12. The minimum energy required to dissociate H_2O into H_2 and O_2 is 1.23 V. It is possible to use a carbon anode and produce CO_2 instead of O_2 . Calculate the minimum cell potential for such a cell.



Note: The actual voltage required is from 0.85 to 1.0 V. Give some reasons for the discrepancy between the calculated and actual values (Fuel 58 705 (1979)).

13. Consider an automobile with an internal combustion engine running on hydrogen which can somehow be stored for a modest run of 50 km. The hydrogen is prepared by the electrolysis of water (in one cell at about 2.5 V) during the night (from 10:00 p.m. to 7:00 a.m.). What would be the required current? Make the following assumptions: (1) heat of combustion of gasoline and hydrogen is given in Table 6.8; (2) the automobile has the efficiency of the new generation of cars, namely, 14 km/L gasoline; and (3) the efficiency of the hydrogen-driven vehicle is related by its comparable heat of combustion to the gasoline efficiency.

Note: Do not be surprised by the large current that is necessary.

14. An ICE vehicle has been described running on H_2 produced on board the vehicle by the reaction of an Al wire with $\text{KOH}/\text{H}_2\text{O}$. Assume that the vehicle is the same one as in Exercise 9.14. Calculate the mass of Al required for the 50-km trip.
15. Calculate the standard cell potential for the Ti/Fe flow battery where

$$\mathcal{E}^\circ_{\text{Ti}^{4+}/\text{Ti}^{3+}} = 0.04 \text{ V}$$

$$\mathcal{E}^\circ_{\text{Fe}^{3+}/\text{Fe}^{2+}} = 0.771 \text{ V}$$

16. Calculate the RI drop of a lead–acid battery (in which the internal resistance is $0.01052 \, \Omega$) when it cranks an engine drawing 200A.
17. Estimate the amount of Glauber’s salt needed to keep a lead–acid battery pack from cooling to 0°C if the outside temperature drops to -40°C . The excess heat for charging the 40-kW power supply will be insulated with 8 cm of Styrofoam. Assume that the volume of the battery pack is 0.3 m^3 , its area is 2.5 m^2 , and its heat capacity is 3 kJ/K . The thermal conduction of the polystyrene foam is $0.0003 \text{ J s}^{-1} \text{ cm}^{-1} \text{ K}^{-1}$. Assume that the EV is stored at work from 8:00 a.m. to 6:00 p.m. at -40°C .
18. From (9.6) and (9.7), calculate the ratio of CO_2/CO produced when TiC is electrolytically machined.

Note: $Z = 6.6$.

Further Reading

- Schmickler W (2010) Interfacial electrochemistry, 2nd edn. Springer, London
- Zinola CF (ed) (2010) Electrocatalysis, vol 149, Computational experimental & industrial aspects. CRC Press, Boca Raton
- Smil V (2010) Energy myths and realities. Bringing science to the energy policy debate. The AEI Press, Washington, DC
- Bard AJ et al (eds) (2010) Electroanalytical chemistry, vol 23. CRC Press, Boca Raton
- Ceroni P et al (eds) (2010) Electrochemistry of functional supramolecular systems. Wiley, Hoboken
- Domenech-Carbo A (2010) Electrochemistry of porous materials. CRC Press, Boca Raton
- Koper M (ed) (2009) Fuel cell catalysis: a surface science approach. Wiley, Hoboken
- Plieth W (2008) Electrochemistry for material science, corrosion & protection. Elsevier, Amsterdam
- Wendt H, Kreysa G (1999) Electrochemical engineering. Springer, New York
- Society of Automotive Engineers (1999) Fuel cell power for transportation. SAE, Warrendale
- Koppel T (1999) Powering the future, the Ballard fuel cell and the race to change the world. Wiley, New York
- Bereny JA (ed) (1996) Battery performance, research and development. Business Technology Books, Orinda

13. Turrentine T, Kurani K (1996) The household market for electric vehicles. Business Technology Books, Orinda
14. Kordesch K, Simader G (1996) Fuel cells and their applications. VCH Pubs, New York
15. Linden D (1996) Handbook of batteries, 2nd edn. McGraw-Hill, New York
16. Saxman D, Grant S (eds) (1995) Batteries and EV industry review. BCC Press, Norwalk
17. Blomen LJ, Mugerwa MN (eds) (1994) Fuel cell systems. Plenum Press, New York
18. Staff OECD (1994) Electric vehicles: performance and potential. OECD, Washington, DC
19. Pletcher D, Walsh FC (1994) Industrial electrochemistry, 2nd edn. Chapman and Hall, London
20. Brant B, Leitman S (1993) Build your own electric vehicle. TAB, New York
21. Koryta J, Dvorak J (1987) Principles of electrochemistry. Wiley, New York
22. Rieger PH (1987) Electrochemistry. Prentice-Hall, Englewood Cliffs
23. Chowdari BVR, Radhakrishna S (eds) (1986) Materials for solid state batteries. World Scientific, Singapore
24. Rand DAJ, Bond AM (eds) (1984) Electrochemistry: the interfacing science. Elsevier, New York
25. Vincent CA (1982) Modern batteries. Edward Arnold, London
26. Unnewehr LE, Nasar SA (1982) Electric vehicle technology. Wiley, New York
27. Barak M (ed) (1980) Electrochemical power sources. Peter Peregrinus Ltd., New York
28. Graham RW (1978) Primary batteries, recent advances. Noyes Data Corp., Park Ridge
29. Antropor LI (1977) Theoretical electrochemistry. MIR Publishers, Moscow
30. Palin GR (1969) Electrochemistry for technologists. Pergamon Press, Oxford
31. Lyons EH Jr (1967) Introduction to electrochemistry. Heather and Co., Boston
32. Potter EC (1956) Electrochemistry—principles and application. Clever-Hume Press, London
33. E.V. Association of America <http://www.evaa.org/Canadian> Electric Vehicle Ltd., <http://www.canev.com>
34. Electrochemistry lecture notes,
35. <http://www.chem.ualberta.ca/courses/plambeck/pl02/p0209x.htm>
36. <http://chemed.chem.purdue.edu/genchem/topicreview/bp/ch20/electroframe.html>
37. <http://edu.cprost.sfu.ca/rhIogan/electrochem.html>
38. <http://www.chem1.com/CB1.htm>
39. Help files for Electrochemistry <http://www.learn.chem.vt.edu/tutorials/electrochem/>
40. Batteries <http://www.panasonic.com/>
41. Batteries <http://www.varta.com/>
42. All about batteries <http://www.howstuffworks.com/battery.htm>